Growth and dissolution of CdS nanoparticles in glass

2001 J. Phys.: Condens. Matter 13 425

(http://iopscience.iop.org/0953-8984/13/3/305)

INSTITUTE OF PHYSICS PUBLISHING JOURNAL OF PHYSICS: CONDENSED MATTER

J. Phys.: Condens. Matter **13** (2001) 425–431 www.iop.org/Journals/cm PII: S0953-8984(01)13916-0

Growth and dissolution of CdS nanoparticles in glass

T M Hayes, L B Lurio[1] and P D Persans

Physics Department, Rensselaer Polytechnic Institute, Troy, NY 12180-3590, USA

Received 16 May 2000, in final form 23 October 2000

Abstract

We report and analyse x-ray absorption spectroscopy of the Cd K edge of CdS-doped glass during growth and dissolution of CdS nanoparticles. Average particle size is deduced from a combination of x-ray and optical spectroscopies. We propose a simple thermodynamic model in which the limiting reactant is in only two environments, either dissolved in the glass or in CdS particles. In this model, the time- and temperature-dependent concentration of Cd dissolved in the glass is related to the total concentrations of Cd and S, the equilibrium solubility of the limiting reactant, and the average CdS particle size.

1. Introduction

Semiconductor nanocrystals exhibit remarkable crystallite-size-related stability and optical effects [1–3]. For example, quantum confinement of electrons and holes leads to a blue shift of the optical absorption edge of CdS particles by several tenths of an electron volt when particle size is varied from several nanometres down to a few nanometres [4]. Precipitation in silicate glass is a commercially established approach to the bulk production of optically useful nanoparticles in a robust, stable form [5, 6]. Better control of particle-size distribution and composition in such particle/glass composites will lead to improved optical properties. Such control requires an understanding of phase segregation and dissolution on a molecular scale.

The growth of CdS semiconductor particles in a glass matrix is based on a thermodynamic process of precipitation from a supersaturated solution. With glasses, the supersaturated solution can be formed by dissolving the reactants in the liquid glass at high temperature and then quenching. The concentration of reactants available for particle formation is limited by supply and reactant solubility in the high-temperature melt. In a 'typical' manufacturing process, the melt temperature is 1300–1450 °C. Particles are grown by diffusion-limited precipitation at temperatures from 600 to 800 °C.

We have employed x-ray absorption spectroscopy (XAS) to study the local bonding of Cd atoms in borosilicate glasses doped with Cd and S after heat treatment at temperatures from 550 to 900 °C. Varying temperature and time can lead to CdS particles with average sizes from a few to several nanometres, with higher temperatures and longer times corresponding to larger particles (until dissolution occurs). Optical absorption and resonant Raman spectroscopies are used to characterize particle size and composition [7].

[1] Presently at Massachusetts Institute of Technology.

0953-8984/01/030425+07$30.00

2. Experimental details and results

The starting material is a glass consisting of SiO_2:B_2O_3:Na_2O:CaO:K_2O:ZnO in the approximate ratios 73:13:6:4.5:2:0.4, as determined by x-ray fluorescence, XAS, and electron microprobe analysis, and doped with 0.1 wt% CdS. As received ('unstruck'), the glass had been homogenized in the melt, quenched, and heat treated to initiate nucleation. It was a pale yellow-green colour in transmission. We subjected 35 × 5 × 2 mm slices of this starting material to isothermal heat treatment for intervals between 0.25 and 14 h.

All of the samples were characterized using optical absorption spectroscopy. Representative spectra are shown in figure 1. The bulk band gap of CdS is 2.45 eV at room temperature. The unstruck glass is characterized by a very gradual onset of absorption starting at ∼2.9 eV. Most of the blue shift of the optical edge is due to quantum confinement. The spectrum evolves monotonically with heat treatment at 625 °C to one characterized by a well-defined peak at ∼3.3 eV (0.25 to 1 h), consistent with an average particle diameter $d \approx 3$ nm. For heat treatment times greater than one hour at 625 °C, the peak evolves into a shoulder and the edge shifts slowly down to ∼2.75 eV. After 14 h at 625 °C the spectrum is characterized by a relatively sharp edge beginning at 2.75 eV (and no peak), consistent with $d > 4$ nm. Treatment at higher temperatures leads to a faster evolution of the peak and edge and can reduce the edge position after a 14 h treatment to ∼2.6 eV. The ∼0.15 eV residual blue shift is due to the substitution of a small amount of Zn for Cd in the particles, as we will discuss below.

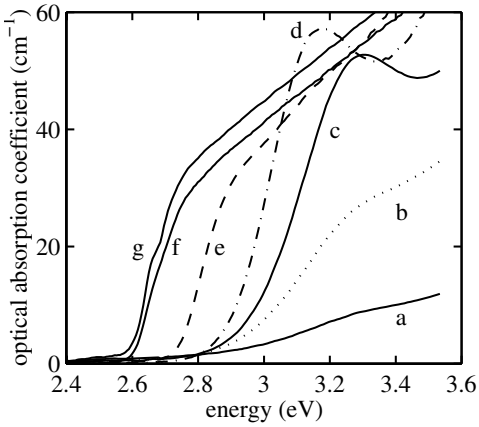

Figure 1. The optical absorption coefficient, plotted against the photon energy, for CdS-doped glass samples heat treated for various temperatures and times: (a) as received; (b) 0.25 hour at 625 °C; (c) 0.5 hour at 625 °C; (d) 1 hour at 625 °C; (e) 14 hours at 625 °C; (f) 14 hours at 700 °C; (g) 14 hours at 725 °C.

We measured the XAS spectra at the Cd K edge for these samples using fluorescence detection. The data were acquired at 20 K using a Si(220) 'two-bounce' monochromator on beamlines 4-2 and 10-2 at the Stanford Synchrotron Radiation Laboratory. Our optics yielded a measured resolution of 12 eV FWHM at the Cd K edge. The XAS spectra were reduced and analysed using standard techniques [8]. Numerical analysis of the spectra using real-space signatures calculated by FEFF3 [9] or extracted from the CdS data yielded the Cd nearest-neighbour coordinations summarized in figure 2. We note that the first-neighbour coordination deduced from XAFS is insensitive to long-range order [8].

In all the samples, both oxygen and sulphur were found as the nearest neighbours of Cd, at distances of 0.228 and 0.252 nm, respectively. Due to the significant differences in the

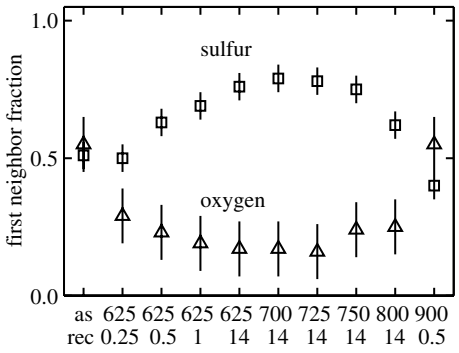

Figure 2. First-nearest-neighbour coordination of Cd atoms in a Cd- and S-doped borosilicate glass after heat treatment at temperatures (in °C) and for times (in hours) as shown.

bonding of these elements to Cd, we presume this to represent a mixture of sites coordinated with either six O or four S. Under that assumption, the 'first-neighbour fraction' shown in figure 2 is calculated by dividing the sulphur or oxygen first-neighbour signal for various heat treatments by the first-neighbour signals measured for CdS and CdO.

In the as-received unstruck sample, the nearest neighbours of Cd are consistent with a 50:50 mixture of (6)O and (4)S sites. It is interesting to note that we observe 50% average coordination of Cd to S in the XAS even when there is only weak optical absorption in the energy range from 2.5 to 4 eV. This suggests that the CdS bonds in this material are in clusters smaller than 2 nm in diameter that would give an optical signature only at higher energies. At the heat treatment temperatures, these small clusters, as well as Cd bonded to O, are unstable with respect to accretion onto larger CdS particles. The growth of the optical absorption peak at 3.3 eV with heat treatment at 625 °C is due to an increase in the number of CdS nanoparticles, with a distribution of diameters with an average of ∼3 nm [6]. At the same time, the average Cd–S coordination increases. After heat treatment at 625 °C for 14 h, the average Cd coordination becomes a 75:25 mixture, favouring S, and the average particle diameter is larger than ∼4 nm. For a 14 h treatment at 700 to 725 °C, the S:O ratio rises slightly to a maximum value of ∼80:20. At heat treatment temperatures above 750 °C the S:O first-neighbour ratio begins to decrease, indicating a shift in the thermodynamic balance between Cd–S and Cd–O. In addition, the magnitude of the Cd–Cd second-neighbour peak decreases, indicating decreasing order in the CdS nanoparticles [10].

3. Discussion

We assume, as the XAFS neighbour data indicate, that the limiting reactant is in two primary environments, either dissolved in the glass host or concentrated in CdS particles. We analyse the concentration of CdS deduced from the first-nearest-neighbour coordination of Cd as follows. If C_{lim} is the concentration of limiting reactant, C_{Cd} is the total concentration, and $C(t)$ is the time-dependent concentration of limiting reactant dissolved in the glass, then the Cd–S coordination C_{norm}, normalized to four S neighbours per Cd dopant atom, will be

$$C_{\mathrm{norm}} = \frac{C_{\mathrm{lim}}}{C_{\mathrm{Cd}}}\left(1 - \frac{C(t)}{C_{\mathrm{Cd}}}\right). \tag{1}$$

We expect, in the equilibrium limit (large R or long time), the Cd–S bond fraction to become

$$C_{\mathrm{norm}} = \frac{C_{\mathrm{lim}}}{C_{\mathrm{Cd}}}\left(1 - \frac{C_{\mathrm{e}}}{C_{\mathrm{Cd}}}\right) \tag{2}$$

where $C_{\mathrm{e}} = C_{00}\exp(-E_{\mathrm{s}}/kT)$ is the solubility of the limiting reactant in the glass.

For $T > 700\ ^{\circ}$C the Cd–S bond fraction reaches a steady state after only a few minutes at a particular temperature. The direct XAFS measurements of the Cd–S bond fraction for such samples are plotted as the squares in figure 3.

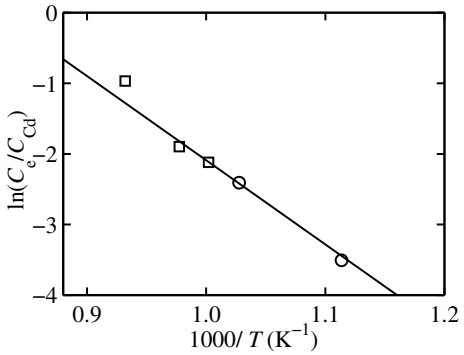

Figure 3. The logarithm of the equilibrium concentration C_e plotted against the inverse of the heat treatment temperature. Points marked by squares are deduced directly from XAS measurements and equation (2). Points marked by circles are deduced from R-dependent fits in figure 5—see later.

For lower-temperature heat treatments, the XAFS Cd–S bond concentration evolves with time. Homogeneous nucleation and ripening theories predict a simple relationship among the minimum stable particle size (critical radius) for CdS, R_C, the equilibrium solubility of the reactant, and the reactant concentration in the glass [6, 11, 12]. In the following, we develop relationships for the temperature and time dependence of these quantities that will allow us to deduce the equilibrium concentrations.

During homogeneous nucleation and ripening, R_C is determined by the balance between volume energy and surface tension:

$$R_C = 2\sigma/\Delta G_V$$

where σ is the effective surface energy per unit area and ΔG_V is the free-energy change between 'dissolved' reactant and solid CdS (per unit CdS crystal volume). We have previously found a relatively small surface energy of <0.15 N m^{-1} from XAS measurements [13]. The free-energy change per unit crystal volume depends on the concentration of the dissolved reactant:

$$\Delta G_V = -(kT/V)\ln(C(t)/C_e).$$

Finally, $C(t)$ will be the lesser of the total limiting reactant, C_0, and the fraction determined by the free energy:

$$C(t) = \text{lesser}\left\{\begin{array}{l} C_0 \\ C_{00}\exp\left(\dfrac{-E_s}{kT}\right)\exp\left(\dfrac{2\sigma V}{kTR_C(t)}\right). \end{array}\right. \tag{3}$$

Measurement of the particle radius from the optical spectrum alone is complicated in this system by the inclusion of a small amount of Zn in the particles [14]. We deduce the composition and size distribution by the consistent analysis of LO vibrational mode energies from Raman scattering, the position and shape of the optical absorption edge, and neighbour distances from XAFS at the Cd K edge [6, 7]. A summary of this approach follows.

The lowest-energy optical transition and the Raman shift depend, in different ways, on particle composition, quantum confinement, and strain. Strain in these systems is small [13] so we neglect it here. For particles of radius $2 < R < 6$ nm, the empirical relationship

$$E_G(R) - E_G(\text{bulk}) \simeq 1.7/R^2 \tag{4}$$

yields a satisfactory agreement with the literature on the shift of the band gap of CdS with size (± 20 meV or ± 0.3 nm) [15]. Substitutional incorporation of Zn for Cd produces an increase in the band gap E_G of wurtzite structure $(ZnS)_x(CdS)_{1-x}$ that can be empirically fitted with [16] $E_G(x) = 2.45 + 0.705x + 0.603x^2$. Incorporation of Zn also causes a shift of the LO phonon Raman energy, empirically given by $\omega(x) = 303 + 91.4x - 44.2x^2$ for $x < 0.2$ [16]. For particles in this size range, the shift in the Raman peak with size is relatively small.

The Raman peak position can be experimentally determined to ± 0.5 cm^{-1} [7], yielding uncertainty in x of ± 0.005, which leads to uncertainty in E_B of 5 meV, small compared to the uncertainty of $\sim$20 meV in the measurement of the shift in the band gap. The shift in the excitation energy can then be used in equation (4) to deduce the particle radius. The combination of uncertainties in the fit to the literature, the measurement of the shift, and the composition leads to uncertainty in R of ± 0.4 nm for $R = 6$ nm and ± 0.1 nm for $R = 2$ nm.

The width of the size distribution is deduced by simulating the lowest-energy peak in the optical absorption spectrum with the sum of a distribution of narrow peaks [6]. The distribution from curves like c and d in figure 1 is consistent with a Gaussian of standard deviation of 13% in size about the average. For longer times, the distribution broadens to a halfwidth at half-maximum of $\sim$25%.

At lower temperatures (<800 °C), the average particle radius and the Cd–S concentration are observed to vary with time. During ripening, the critical radius is expected to increase according to $R(t) = R_0 + (4\alpha D/9)t^{1/3}$ where R_0 is the average radius of particles at the start of ripening, $\alpha = 2\sigma v^2 C_e/kT$, and D is the diffusion coefficient of the limiting reactant [12,17]. In figure 4 we have plotted the average particle radius against time for two heat treatment temperatures. We observe that for longer times the slope of $\log(R)$ against $\log(t)$ approaches 1/3 (dashed line), consistent with Lifshitz–Slyozov ripening. Ripening is also consistent with the significant change in CdS/CdO bonding observed in figure 2.

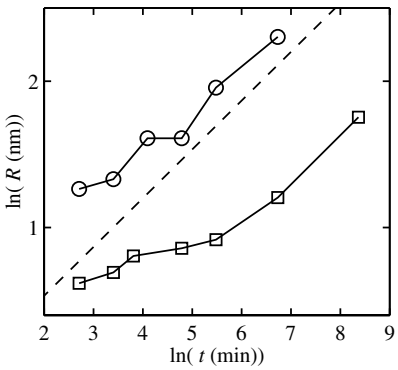

Figure 4. The logarithm of the average particle radius, deduced by combining optical absorption spectra and vibrational energies, plotted against the logarithm of the heat treatment time at 625 °C (squares) and 700 °C (circles). The dashed line corresponds to a slope of 1/3 (ripening model).

In figure 5 we plot the Cd–S coordination against particle radius for heat treatment at 625 °C and 700 °C. The two lines result from equations (1) and (3) with $2\sigma V/k$ of 4.4×10^{-3} nm K, $C_{lim} = 0.9$, and $C_e/C_{Cd} = 0.03$ for 625 °C and $C_e/C_{Cd} = 0.1$ for 700 °C. The observations

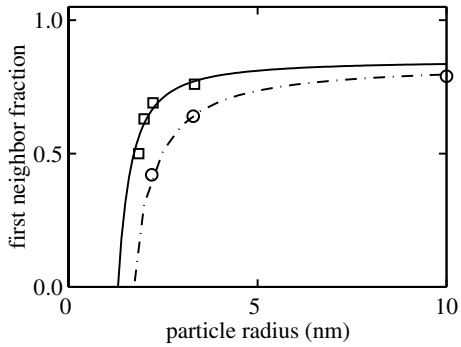

Figure 5. Fractional S first-neighbour coordination of Cd, plotted against average particle radius for heat treatment for various times at 625 °C (squares) and 700 °C (circles). Lines are fits using equations (1) and (3). The fit parameters are given in the text.

that the large-R asymptote is less than one and is nearly the same for 625 and 700 °C suggests that the limiting reactant is S or that 10% of the Cd is able to find a site with lower energy. The increase in C_e/C_{Cd} with temperature is consistent with solubility increasing with temperature.

We find that the concentration is within a few per cent of its asymptote after several hours at 625 °C and after several minutes at 700 °C. It should approach the asymptote faster at higher temperatures, so we use 0.90 minus the coordination fraction as a measure of C_e/C_{Cd}. These data are added to figure 3 as circles. A least-squares straight-line fit to $\ln(C_e)$ plotted against inverse temperature in figure 3 yields an activation energy of $E_s = 0.55$ eV for the temperature range from 625 to 900 °C. This activation energy is consistent with expected chemical bond energies, and allows us to predict the solubility of the limiting reactant at high temperature. We also observe in figure 5 that complete dissolution of CdS particles is expected at ∼950 °C, consistent with the absence of optical absorption below 2.9 eV in glass quenched from above 950 °C.

Although a glass may be heat treated at a high temperature T_M, the condition of the quenched glass will reflect some fictive temperature T_f which may be higher or lower than the treatment temperature. If the heat treatment temperature is high enough that the glass achieves equilibrium within the treatment time, then the fictive temperature on quenching will be lower than the heat treatment temperature. Different measured quantities will have different fictive temperatures. If the quench rate is high enough, the fictive temperature will be close to the heat treatment temperature. The simple activated behaviour of C_e indicates that our quench rates of 10 °C s^{-1} are fast enough that $T_f \sim T_M$ up to 900 °C.

4. Summary

We have quantitatively analysed the changes in atomic scale bonding of Cd atoms due to heat treatment of glass doped with $\sim 1.2 \times 10^{19}$ Cd cm^{-3}. The as-received glass is quenched from the melt at ∼1400 °C and heat treated at ∼500 °C to reduce stress. In this as-received glass, about 50% of the Cd atoms are found in a CdS-like environment. The absence of significant optical absorption below 3.5 eV indicates that these CdS clusters are smaller than 2 nm in diameter. Heat treatment at 600–900 °C leads to the growth of CdS nanoparticles. For isothermal heat treatment, we observe the progressive replacement of O with S as the nearest neighbour of Cd. The average particle size, deduced from optical measurements, increases with heat treatment time. The evolutions of the particle size with time at 625 °C and

700 °C are consistent with homogeneous nucleation followed by Lifshitz–Slyozov ripening and suggest that a simple thermodynamic model can be used to relate the average particle size to the concentration of available reactants dissolved in the glass. Both the R-dependence of the Cd–S bond fraction and the large-R asymptote of the Cd–S coordination number are measures of the solubility of the limiting reactant in the glass. A fit of our growth and dissolution model to the measurements yields a solubility activation energy for the limiting reactant of 0.55 eV over the temperature range from 625 to 900 °C.

Acknowledgments

We thank Schott Glass Technologies for providing the unstruck doped glass. We gratefully acknowledge support of this research by DOE grant No DE-FG02-97ER45662. The XAS measurements were made at SSRL, which is funded by the DOE Office of Basic Energy Sciences and the NIH Biotechnology Resource Program.

References

[1] Brus L E 1991 *Appl. Phys.* A **53** 465
[2] Alivisatos A P 1995 *Bull. Mater. Res. Soc.* **20** 14
[3] Schroeder J and Persans P D 1996 *J. Lumin.* **70** 69
[4] Ekimov A I and Onushchenko A A 1982 *Sov. Phys.–Semicond.* **16** 775
[5] Borrelli N F, Hall D, Holland H and Smith D 1987 *J. Appl. Phys.* **61** 5399
[6] Yükselici H, Persans P D and Hayes T M 1996 *Phys. Rev.* B **52** 11 763
[7] Persans P D, Lurio L B, Pant J, Yükselici H, Lian G D and Hayes T M 2000 *J. Appl. Phys.* **87** 3850
[8] Hayes T M and Boyce J B 1982 *Solid State Physics* vol 37, ed H Ehrenreich, F Seitz and D Turnbull (New York: Academic) pp 173–351
[9] Rehr J J, Mustre de Leon J, Zabinsky S I and Albers R C 1991 *J. Am. Chem. Soc.* **113** 5135
[10] Hayes T M, Lurio L B, Pant J and Persans P D 2001 *Solid State Commun.* at press
[11] Gurevich S A, Ekimov A I, Kudryavtsev I A, Lyublinskaya O G, Osinskii A V, Usikov A S and Faleev N N 1994 *Semiconductors* **28** 486
[12] Lifshitz I M and Slyozov V V 1961 *J. Chem. Phys. Solids* **19** 35
[13] Hayes T M, Lurio L B, Pant J and Persans P D 2001 *Phys. Rev.* B at press
[14] Persans P D, Lurio L B, Pant J, Lian G D and Hayes T M 2001 *Phys. Rev.* B at press
[15] Persans P D and Stokes K L 1997 *Handbook of Nanophase Materials* ed A Goldstein (New York: Dekker) pp 271–316
[16] Madelung O, Schulz M and Weiss H 1982 *Landolt–Börnstein New Series* Group III, vol 17 (Berlin: Springer)
[17] Potter B G and Simmons J H 1988 *Phys. Rev.* B **37** 10 838